21. Because of the parallel plate (rather than crossed cylinder) geometry, the Derjaguin approximation commonly used in reporting surface forces measurements (*4–6*) did not apply. For this reason, we report $P_\perp$, force normalized by the contact area.
22. J. Klein and P. F. Luckham, *Nature* **308**, 836 (1984).
23. M. Doi and S. F. Edwards, *The Theory of Polymer Dynamics* (Oxford Univ. Press, New York, 1986).
24. J. F. Douglas and J. B. Hubbard, *Macromolecules* **24**, 3163 (1991).
25. We are indebted to J. F. Douglas, J. D. Ferry, G. Reiter, and K. Schweizer for comments and discussions and to S. J. Clarson for donating the PPMS samples used in this study. H.-W.H. acknowledges partial support from grant NSF-MSS-92-02143. We acknowledge primary support of the National Science Foundation through the Materials Research Laboratory at the University of Illinois, grant NSF-DMR-89-20538.

31 July 1992; accepted 5 October 1992

---

# Direct Observation of ClO from Chlorine Nitrate Photolysis

Timothy K. Minton, Christine M. Nelson, Teresa A. Moore, Mitchio Okumura

**Chlorine nitrate photolysis has been investigated with the use of a molecular beam technique. Excitation at both 248 and 193 nanometers led to photodissociation by two pathways, $ClONO_2 \rightarrow ClO + NO_2$ and $ClONO_2 \rightarrow Cl + NO_3$, with comparable yields. This experiment provides a direct measurement of the ClO product channel and consequently raises the possibility of an analogous channel in ClO dimer photolysis. Photodissociation of the ClO dimer is a critical step in the catalytic cycle that is presumed to dominate polar stratospheric ozone destruction. A substantial yield of ClO would reduce the efficiency of this cycle.**

The mechanisms of polar ozone depletion are well established (*1*). The main catalytic cycle is believed to be (*1, 2*):

$$\begin{aligned} ClO + ClO + M &\rightarrow ClOOCl + M \\ ClOOCl + h\nu &\rightarrow ClOO + Cl \\ ClOO + M &\rightarrow Cl + O_2 + M \\ 2(Cl + O_3 &\rightarrow ClO + O_2) \\ \hline \text{Net: } 2O_3 &\rightarrow 3O_2 \end{aligned}$$

The photochemical step in this cycle plays the pivotal role of releasing atomic chlorine from the ClO dimer. This step requires that the Cl–O bond [enthalpy of reaction $\Delta H^\circ(0\ \mathrm{K}) = 84$ kJ/mol] breaks preferentially over the weaker O–O bond [$\Delta H^\circ(0\ \mathrm{K}) = 67$ kJ/mol] (*3*), and it has been rationalized by the argument that excitation of an $n \rightarrow \sigma^*$ transition localized on the ClO chromophore leads to selective dissociation of the Cl–O bond. In this report, we describe an investigation of the photodissociation of chlorine nitrate ($ClONO_2$) that refutes this argument and thus indirectly raises questions about the photolysis products from ClOOCl.

The notion of selective Cl–O bond fission has evolved from earlier observations that $ClONO_2$ dissociates almost exclusively to Cl and $NO_3$ (*2*). $ClONO_2$ has been studied extensively because of its importance as a reservoir species for active chlorine and $NO_x$ in the stratosphere (*4*). Earlier studies (*5–11*) reported the dominant channels to be

$$ClONO_2 \rightarrow Cl + NO_3$$
$$ClONO_2 \rightarrow ClONO + O$$

The $\Delta H^\circ(0\ \mathrm{K})$ of these reactions are 167 kJ/mol and 280 kJ/mol respectively. While discrepancies exist in the relative yields for these channels, none of the earlier studies reported dissociation of the weakest bond,

$$ClONO_2 \rightarrow ClO + NO_2$$

which has a $\Delta H^\circ(0\ \mathrm{K})$ of 109 kJ/mol, because the indirect methods used to detect ClO failed to reveal its presence. In an evaluation of data for use in stratospheric modeling, DeMore *et al.* (*12*) preferred the results of Margitan's experiment (*10*), which was a direct study of $ClONO_2$ photolysis at both 266 and 355 nm. With the use of resonance fluorescence to detect Cl atoms and O atoms in a flow cell, Margitan measured Cl and O quantum yields of 0.9 ± 0.1 and 0.1 ± 0.1, respectively. These results have gained broad acceptance.

Although Margitan's experiment lends support to the picture of a transition localized on the ClO chromophore over an argument based on bond energies, the discrepancies among the earlier experiments and their lack of detection of ClO impart uncertainty to the conclusion that the ClO chromophore can be viewed as a distinct entity. Nevertheless, the ultraviolet absorption spectrum (*13*) of $ClONO_2$ shows two overlapping and structureless absorption features that are reminiscent of absorptions in the two chromophores that make up the molecule. The feature with a peak near 215 nm may correspond to an $n \rightarrow \sigma^*$ transition localized on the ClO moiety (*2*), whereas the rise near 190 nm may correspond to a $\pi \rightarrow \pi^*$ transition on the $NO_2$ group (*14*). Within the confines of this simple picture, each of two wavelengths available with an excimer laser, 248 and 193 nm, should excite one of the respective transitions.

We examined the possibility of bond-selective photolysis of the ClO chromophore in a molecular beam study of the photodissociation of $ClONO_2$ at 248 and 193 nm. With the use of molecular beam methods, we could directly detect the photofragments, identify primary and secondary dissociation channels, and quantitatively determine the relative product yields. We detected both ClO and Cl photoproducts (but not ClONO), and we determined the relative yields of these two products by calibrating the detector sensitivity for ClO and Cl with a $Cl_2O$ photolysis experiment at 308 nm.

Our experiment utilized the technique of photofragment translational energy spectroscopy (*16*) and was performed with a universal crossed molecular beams machine (*17*) in which a pulsed excimer laser beam was substituted for one of the molecular beams (Fig. 1). The laser beam was focused to a spot size of ~0.1 cm$^2$ where it crossed a molecular beam. The laser fluence was varied over one order of magnitude to check for a power dependence of the various signals observed. Only photoproducts that recoil away from the molecular beam direction can be detected by the mass spectrometer detector, which can be rotated about the molecular beam–laser interaction zone. The distance from the interaction

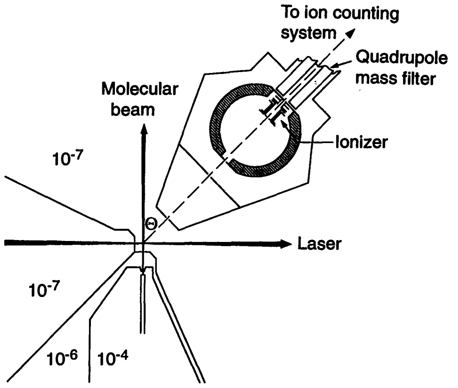

**Fig. 1.** Schematic diagram of the molecular beam photodissociation experiment. The numbers correspond to pressures in Torr for the various regions. Θ is the detector angle.

---

T. K. Minton, Jet Propulsion Laboratory, Mail Stop 67-201, California Institute of Technology, 4800 Oak Grove Drive, Pasadena, CA 91109.
C. M. Nelson, T. A. Moore, M. Okumura, Arthur Amos Noyes Laboratory of Chemical Physics, Mail Stop 127-72, California Institute of Technology, Pasadena, CA 91125.

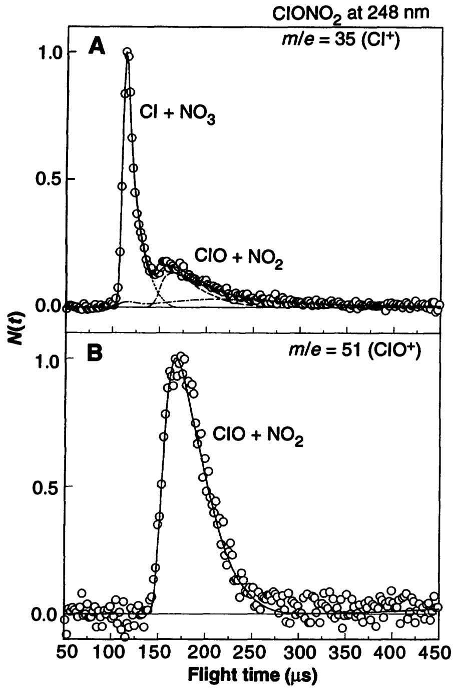

**Fig. 2.** TOF distributions $N(t)$ in arbitrary units (*30*) at a detector angle of 30° for (**A**) $Cl^+$ and (**B**) $ClO^+$ fragments from $ClONO_2$ photodissociation at 248 nm. Fits to distributions are predicted by optimized translational energy and angular distributions $P(E_T)$ and $w(\theta)$, respectively. The broad, underlying component in (A) is calculated with the use of a procedure (*31*) to model secondary photodissociation of the primary ClO photoproduct.

zone to the electron bombardment ionizer of the mass spectrometer was 34.1 cm. Time-of-flight (TOF) distributions for each pertinent photofragment mass-to-charge ratio ($m/e$) were collected at many detector angles as a function of time from the laser pulse. Analysis of TOF and angular distributions was carried out with a standard technique (*16*) in which a laboratory distribution is predicted by first estimating center-of-mass (c.m.) translational energy and angular distributions and then transforming them to the laboratory reference frame. The initial c.m. distributions are varied until a good match with all the observed laboratory data is obtained.

We synthesized chlorine nitrate from the reaction of $Cl_2O$ with $N_2O_5$ and then purified it (*18*). $Cl_2O$ from the first step in the $ClONO_2$ synthesis was used for the $Cl_2O$ calibration experiment. We formed molecular beams by bubbling He through $ClONO_2$ at −60°C or through $Cl_2O$ at −74°C and expanding the mixture at a total pressure of 200 Torr through a 0.10-mm-diameter quartz nozzle held at 5°C. Both beams had a nominal velocity of 1.3 km/s, as determined by beam TOF distributions taken with the aid of a chopper wheel. The resulting density of $ClONO_2$ or $Cl_2O$ in the interaction region was $\sim 10^{11}$ cm$^{-3}$. The presence of clusters and impurities in the molecular beams had no bearing on the results (*19*).

The results from excitation at both 248 and 193 nm were analogous, although the dynamics differed, and we use the 248-nm data to illustrate the key elements of the experiment and analysis.

Two components in the TOF distribution at $m/e = 35$ ($Cl^+$) (Fig. 2) indicate that there were two distinct dissociation channels. At $m/e = 51$ ($ClO^+$), only one peak appeared. We assigned this peak to ClO from the ClO + $NO_2$ channel and not to ClONO from the ClONO + O channel (*20*). Given the 4-μs difference in ion flight times, the ClO peak matches the slow peak in the TOF distribution at $m/e = 35$ almost exactly (*21*). Thus, the slow peak at $m/e = 35$ must be the result of cracking of ClO to $Cl^+$ in the ionizer. The most likely dissociation channel that was responsible for the fast peak at $m/e = 35$ is Cl + $NO_3$.

On the basis of the conclusion that the signal at $m/e = 51$ comes from ClO + $NO_2$, we derived a c.m. translational energy distribution $P(E_T)$ and angular distribution $w(\theta)$ for that channel (*21a*), which gave the fit shown in Fig. 2B. These distributions were then used to fit the slow peak at $m/e = 35$. Knowing the shape of the slow component allowed us to derive a second set of $P(E_T)$ and $w(\theta)$ distributions for the Cl + $NO_3$ channel from the fast peak.

We checked our assignments of the two dissociation channels by using the $P(E_T)$ and $w(\theta)$ distributions to predict the shapes of the TOF distributions for the momentum-matched counter fragments, $NO_2$ and $NO_3$, (Fig. 3). We did not observe any signal at the $NO_3$ parent mass, as $NO_3$ apparently fragmented in the ionizer, but the TOF spectrum collected at $m/e = 46$ (Fig. 3A) was fit well with the prediction from the Cl + $NO_3$ $P(E_T)$ and $w(\theta)$ distributions except for a slight discrepancy on the slow side. This generally good match indicated that the peak at $m/e = 46$ arose solely from $NO_3$ photoproducts that fragmented to $NO_2^+$ in the ionizer. The apparent lack of signal on the slow side of the TOF distribution is the result of secondary dissociation of slowly recoiling $NO_3$ photofragments that were highly internally excited and that dissociated before reaching the detector (*22*). The TOF distribution at $m/e = 30$ ($NO^+$) exhibits a peak that is superimposed on a broad background. The peak shape could not be fit from $P(E_T)$ and $w(\theta)$ distributions for either the ClO + $NO_2$ or the Cl + $NO_3$ channels alone; however, the sum of contributions from each channel (*23*) did match the peak shape. Hence, both $NO_3$ and $NO_2$ photofragments contributed to the peak at $m/e = 30$. The broad background is the manifestation of the secondary dissociation of $NO_3$ into $NO_2$ + O and NO + $O_2$. Although the counterfragment TOF distributions were complicated by ionizer fragmentation, overlapping flight times, and secondary dissociation, a full analysis of the dissociation dynamics confirmed our original assignments of the two primary photodissociation channels in $ClONO_2$.

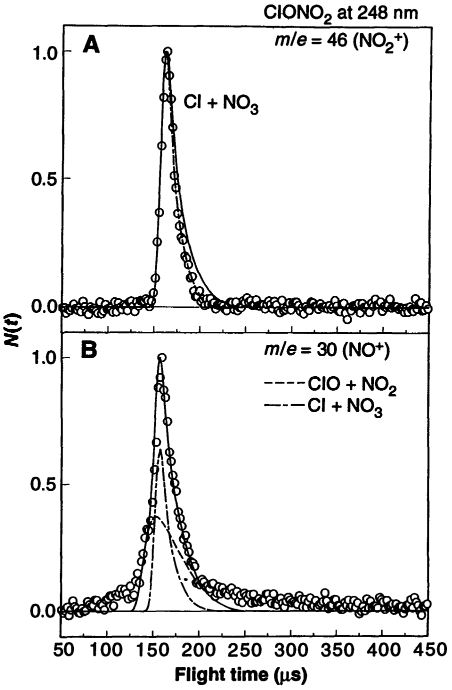

**Fig. 3.** TOF distributions for counterfragments to those whose TOF distributions are shown in Fig. 2.

Study of $Cl_2O$ photodissociation allowed us to calibrate the detection efficiency for Cl and ClO at $m/e = 35$ and thereby determine the branching ratio between the $ClONO_2$ photodissociation channels. We carried out the calibration experiment at 308 nm, where $Cl_2O$ dissociates exclusively to ClO + Cl without the complication of secondary dissociation. The TOF distribution at $m/e = 35$ (Fig. 4A) is analogous to those observed for $ClONO_2$, consisting of a Cl atom component and a ClO component. Even though the Cl:ClO ratio must necessarily be 1:1 in the $Cl_2O$ experiment, the ClO peak at $m/e = 35$ is significantly smaller than the Cl atom peak because only about 25% of the ClO radicals fragment to $Cl^+$ in the ionizer. By deriving $P(E_T)$ and $w(\theta)$ distributions for $Cl_2O$ photodissociation and then scaling two such $P(E_T)$ distributions until the predicted TOF distributions agreed with those observed at $m/e = 35$, we found the ratio of the flux of Cl to ClO detected at $m/e = 35$. This calibration factor had to be corrected slightly because ClO from $ClONO_2$ photolysis at 248 and

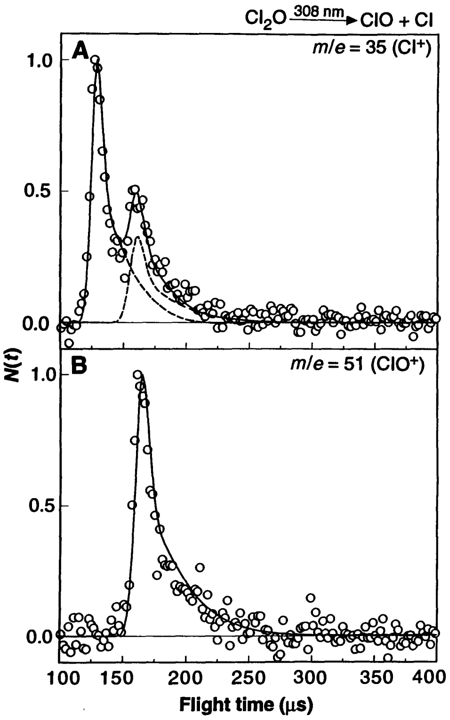

**Fig. 4.** TOF distributions at a detector angle of 30° for $Cl^+$ and $ClO^+$ fragments from $Cl_2O$ photodissociation at 308 nm.

193 nm fragmented more in the ionizer than did ClO from $Cl_2O$ photolysis at 308 nm. We assumed that the ClO ionization cross section for ~160-eV electrons is independent of vibrational energy.

We observed only two primary dissociation channels at each photolysis wavelength (Table 1), and unlike earlier studies, we were able to detect the ClO product and its momentum-matched counterfragment directly in the absence of collisions. A straightforward calibration experiment indicates that the ClO + $NO_2$ channel is indeed an important dissociation pathway (24). Because a small fraction of ClO photodissociated at 248 nm even at the lowest laser power that we used, the ClO yield at 248 nm must be regarded as a lower limit. We saw no direct evidence for the existence of a ClONO + O dissociation channel; however, a yield of ≤0.04 would place ClONO below our detection limit. The results also indicate that O atoms, although not a primary product, can be formed through various secondary dissociation processes.

The discrepancy with earlier gas cell experiments is difficult to reconcile. With the exception of the work by Margitan, the evidence against a significant yield of ClO is not strong (25). Although we cannot resolve the disagreement with Margitan, it is possible that ClO photoproducts went undetected in his experiment. The laser powers used, coupled with the likely hot spots in the 266-nm quadrupled Nd:YAG laser beam, may have led to extensive secondary photolysis of ClO into Cl and O [primarily $O(^1D)$], thus inhibiting detection of $O(^3P)$ atoms and producing an apparent quantum yield near unity for Cl atoms. If ClO products did not photolyze, then they should have been detected by NO titration, but there was not enough published information to evaluate the NO titration measurement. Finally, the discrepancy with our experiment could be explained if the branching ratio differs between 248- and 266-nm photolysis.

**Table 1.** Relative yields of the two primary photodissociation channels in $ClONO_2$ at 248 and 193 nm.

| Dissociation channel | Fraction | |
|---|---|---|
| | 248 nm | 193 nm |
| ClO + $NO_2$ | 0.46 ± 0.08 | 0.36 ± 0.08 |
| Cl + $NO_3$ | 0.54 ± 0.08 | 0.64 ± 0.08 |

The observation that the two photodissociation channels have comparable yields at two distinct wavelengths suggests that strong coupling exists among the excited states of $ClONO_2$; the photolysis of ClOOCl is likely to be equally complex. In essentially a bond-strength analysis, Eberstein (26) argued by analogy with HOOH that ClOOCl should photodissociate to ClO + ClO. Contrary to this argument, Stanton *et al.* (27) calculated that electronic absorptions in ClOOCl near 250 nm involve population of ClO σ antibonding orbitals; this calculation lends support to the idea of selective photolysis of the Cl–O bond. On the other hand, a localized transition does not necessarily imply that Cl–O bond fission should dominate, as branching into the final product channels is governed by nuclear motion on the excited state potential energy surfaces. Laboratory results have apparently confirmed that Cl–O bond fission is the only photodissociation mechanism, but these results are equivocal (28, 29).

In ClOOCl, as in $ClONO_2$, the ClO photoproduct may have been missed in earlier experiments, and there could be two dissociation channels, one producing Cl atoms and one producing ClO. If substantial O–O bond fission does occur, then the ClO dimer mechanism might not be responsible for as much ozone depletion as currently thought. Knowledge of the photochemistry of ClOOCl is vital to the understanding of polar ozone depletion, and our results on $ClONO_2$ and the uncertainties in the experiments on ClOOCl imply that photodissociation of ClOOCl should be reinvestigated.

## REFERENCES AND NOTES

1. J. G. Anderson, D. W. Toohey, W. H. Brune, *Science* **251**, 39 (1991); P. Hamill and O. B. Toon, *Phys. Today* **44** (no. 12), 34 (1991).
2. L. T. Molina and M. J. Molina, *J. Phys. Chem.* **91**, 433 (1987).
3. M. W. Chase, Jr., *et al.*, *J. Phys. Chem. Ref. Data* **14**, 718 (1985); S. Abramowitz and M. W. Chase, Jr., *Pure Appl. Chem.* **63**, 1449 (1991); R. L. Mauldin III, J. B. Burkholder, A. R. Ravishankara, *J. Phys. Chem.* **96**, 2582 (1992).
4. F. S. Rowland, J. E. Spencer, M. J. Molina, *J. Phys. Chem.* **80**, 2711 (1976); *ibid.*, p. 2713.
5. W. S. Smith, C. C. Chou, F. S. Rowland, *Geophys. Res. Lett.* **4**, 518 (1977).
6. J. S. Chang, J. R. Barker, J. E. Davenport, D. M. Golden, *Chem. Phys. Lett.* **60**, 385 (1979).
7. S. M. Adler-Golden and J. R. Wiesenfeld, *ibid.* **82**, 281 (1981).
8. W. J. Marinelli and H. S. Johnston, *ibid.* **93**, 127 (1982).
9. H. D. Knauth and R. N. Schindler, *Z. Naturfor.* **38A**, 893 (1983).
10. J. J. Margitan, *J. Phys. Chem.* **87**, 674 (1983).
11. J. P. Burrows, G. S. Tyndall, G. K. Moortgat, *ibid.* **92**, 4340 (1988).
12. W. B. DeMore *et al.*, "Chemical Kinetics and Photochemical Data for Use in Stratospheric Modeling" (*Publ. 92-20*, Jet Propulsion Laboratory, Pasadena, CA, 1992).
13. L. T. Molina and M. J. Molina, *J. Photochem.* **11**, 139 (1979).
14. Compare with the absorption spectrum (*15*) of $HNO_3$.
15. L. T. Molina and M. J. Molina, *J. Photochem.* **15**, 97 (1981).
16. G. E. Busch and K. R. Wilson, *J. Chem. Phys.* **56**, 3626 (1972); *ibid.*, p. 3638; T. K. Minton, G. M. Nathanson, Y. T. Lee, *ibid.* **86**, 1991 (1987); A. M. Wodtke and Y. T. Lee, *J. Phys. Chem.* **89**, 4744 (1985).
17. Y. T. Lee, J. D. McDonald, P. R. LeBreton, D. R. Herschbach, *Rev. Sci. Instrum.* **40**, 1402 (1969); R. K. Sparks, thesis, University of California, Berkeley (1980).
18. M. Schmeisser, *Inorg. Syn.* **9**, 127 (1967).
19. The $Cl_2O$ beam had a significant $Cl_2$ impurity, but it did not affect the experiment because of its relatively low absorption cross section at 308 nm. (Even if $Cl_2$ did absorb, it would produce a sharp and easily assignable peak in the TOF distribution at *m/e* = 35 because it is a diatomic molecule.) The $ClONO_2$ beam did show some evidence of clusters, both in the beam TOF distributions (signal at *m/e* = 143) and in photofragment TOF distributions (a slow signal corresponding to species whose velocities were close to the molecular beam velocity). In all TOF distributions where dissociation of clusters was suspected of contributing to the signal, the dependence of the signal on the partial pressure of $ClONO_2$ in the beam was used to confirm this assignment. Although both $ClONO_2$ and $Cl_2O$ beams could have contained impurities below the detector sensitivity in the beam TOF distributions, no photofragment signal was detected that could reasonably be assigned to an impurity in the beam.
20. We justify the assignment of the *m/e* = 51 peak on the basis that we observed no signal at the ClONO parent mass; it would be energetically impossible for ClONO to arrive at times shorter than 225 μs at a detector angle of 30°; and the only other peak at *m/e* = 51 that was observable at small angles was shown to arise from cluster dissociation.
21. A broad, underlying component in the TOF distribution at *m/e* = 35 was found to arise from secondary photodissociation of primary ClO photoproducts. This secondary signal was small at large detector angles as a result of a strong anisotropy in the angular distributions of both the primary and secondary processes.

21a. θ is the angle between the electric vector of the laser light and the c.m. recoil direction of the photoproducts (*16*).

22. T. K. Minton, P. Felder, R. J. Brudzynski, Y. T. Lee, *J. Chem. Phys.* **81**, 1759 (1984).
23. A truncated $P(E_T)$ distribution derived from the $m/e = 46$ TOF distribution was used for the Cl + NO$_3$ contribution.
24. From anisotropy in the angular distributions, we found that ClONO$_2$ dissociates rapidly, within a rotational period, producing excited but bound ClO products (at low laser powers). Therefore, the ClO/Cl branching ratios that we observed should also be observed in the stratosphere and in bulk gas phase experiments, where prompt dissociation will occur faster than the mean collision rate.
25. The direct study by Marinelli and Johnston (*8*) found that the NO$_3$ yield, corrected for a revised calibration factor (*11*), is less than 40%, and NO$_2$ and secondary N$_2$O$_5$ products have been detected in steady state (*11*) and static cell (*5, 9*) experiments.
26. I. J. Eberstein, *Geophys. Res. Lett.* **17**, 721 (1990).
27. J. F. Stanton, C. M. L. Rittby, R. J. Bartlett, D. W. Toohey, *J. Phys. Chem.* **95**, 2107 (1991).
28. R. A. Cox and G. D. Hayman [*Nature* **332**, 796 (1988)] collected ultraviolet absorption spectra of ClO, Cl$_2$O, and ClOOCl products from the steady-state photolysis of Cl$_2$O at 254 nm. Accelerated Cl$_2$O loss was attributed to reactions with Cl atoms formed from ClOOCl photolysis. A quantum yield of 3.8 ± 1.6 for Cl atoms from ClOOCl photolysis was extracted by fitting the observations to a multistep kinetic mechanism.
29. M. J. Molina, A. J. Colussi, L. T. Molina, R. N. Schindler, and T.-L. Tso [*Chem. Phys. Lett.* **173**, 310 (1990)] used resonance fluorescence to detect directly Cl atoms following photolysis of ClOOCl at 308 nm in a flow tube, and they reported a Cl atom quantum yield of 1.03 ± 0.12 for the reaction ClOOCl → Cl + ClOO. They detected no ClO with NO titration. Their quantum yield depends on the ratio of the absorption cross sections of ClOOCl at 254 and 308 nm. With the use of the absorption spectrum recommended by DeMore *et al.* (*12*), the Cl + ClOO yield would be 0.6.
30. All TOF distributions shown include the ion flight time, 3.54 $\sqrt{m/e}$ μs.
31. E. J. Hintsa, X. Zhao, Y. T. Lee, *J. Chem. Phys.* **92**, 2280 (1990); X. Zhao, G. M. Nathanson, Y. T. Lee, *Acta Phys.-Chim. Sinica* **8**, 70 (1992).

32. This research was carried out at the Jet Propulsion Laboratory, California Institute of Technology, under contract with the National Aeronautics and Space Administration (NASA). This work was supported by NASA contract NAS 7-918, through the Caltech President's Fund, a National Science Foundation Presidential Young Investigator award (CHE-8957243), the Caltech Consortium in Chemistry and Chemical Engineering [founding members, E. I. duPont de Nemours and Co., Inc., Eastman Kodak Co., and Minnesota Mining and Manufacturing Co.], a Dreyfus Newly Appointed Faculty Award (M.O.), and Department of Education and NASA Fellowships (C.M.N.). We are grateful to Y. L. Yung, S. P. Sander, and R. R. Friedl for helpful discussions and to P. Felder for assistance with the secondary dissociation analysis. Contribution No. 8675, Arthur Amos Noyes Laboratory of Chemical Physics, California Institute of Technology.

6 July 1992; accepted 5 October 1992

---

# Evidence from 12*S* Ribosomal RNA Sequences That Onychophorans Are Modified Arthropods

J. William O. Ballard,* Gary J. Olsen, Daniel P. Faith,
Wendy A. Odgers, David M. Rowell, Peter W. Atkinson

**The evolutionary relationships of the onychophorans (velvet worms) and the monophyly of the arthropods have generated considerable debate. Cladistic analyses of 12*S* ribosomal RNA sequences indicate that arthropods are monophyletic and include the onychophorans. Maximum parsimony analyses and monophyly testing within arthropods indicate that myriapods (millipedes and centipedes) form a sister group to all other assemblages, whereas crustaceans (shrimps and lobsters) plus hexapods (insects and allied groups) form a well-supported monophyletic group. Parsimony analysis further suggests that onychophorans form a sister group to chelicerates (spiders and scorpions) and crustaceans plus hexapods, but this relationship is not well supported by monophyly testing. These relationships conflict with current hypotheses of evolutionary pathways within arthropods.**

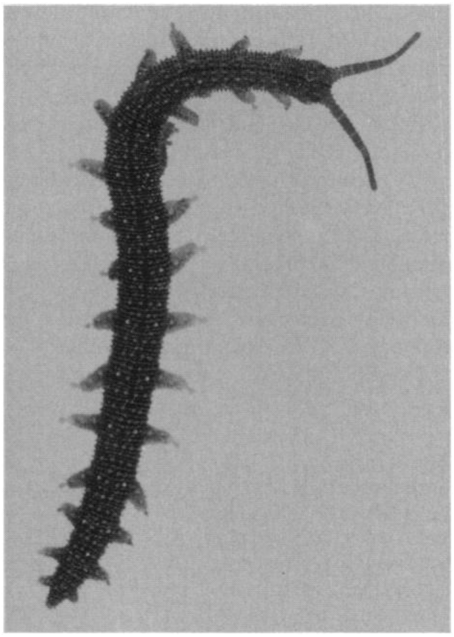

**Fig. 1.** An undescribed oviparous onychophoran species from eastern Australia.

The question of whether arthropods, or jointed foot invertebrates, have a common ancestor has generated debate. Central to this discussion is the phylogenetic position of onychophorans, or velvet worms. These enigmatic invertebrates resemble slugs with legs (Fig. 1), and an early report described them as mollusks (chitons, limpets, and snails) (*1*). They have been described as the missing link between arthropods and annelids (segmented worms) because of physical similarities to both groups. Currently there are four major hypotheses of onychophoran evolutionary relationships (*2–5*) (Fig. 2). On the basis of morphological criteria, these hypotheses group myriapods (millipedes and centipedes) and hexapods (insects and allied groups) together to form the atelocerates. The morphological characteristics used by these models include the presence of anterior tentorial arms, the absence of pretarsal levator muscles, the absence of distinct appendages on the tritocephalic head segment (*6*), and appendage evolution (*7*).

Ultrastructural similarities between the sperm of onychophorans and euclitellates (oligochaetes, branchiobdellids, and leeches) have led to the proposition that onychophorans are more closely related to certain annelids than to arthropods (*2*) (Fig.

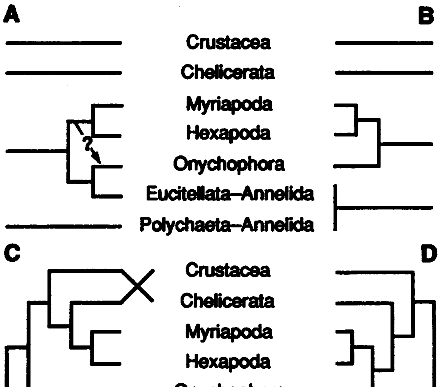

**Fig. 2.** Polyphyletic (A and B) and monophyletic (C and D) hypotheses of arthropod relationships. Polyphyletic hypotheses propose either that (**A**) onychophorans are more closely related to certain annelids than to arthropods (*2*) or (**B**) arthropodization has occurred independently at least three times (*3*). Hypotheses of arthropod monophyly propose onychophorans are either (**C**) primitive (*4*) or (**D**) closely allied to myriapods and hexapods (*5*).

J. W. O. Ballard, W. A. Odgers, P. W. Atkinson, Division of Entomology, Commonwealth Scientific and Industrial Research Organisation (CSIRO), Canberra, ACT 2601, Australia.
G. J. Olsen, Department of Microbiology, University of Illinois, Urbana, IL 61801.
D. P. Faith, Division of Wildlife and Ecology, CSIRO, Lyneham, ACT 2602, Australia.
D. M. Rowell, Department of Botany and Zoology, Australian National University, Canberra, ACT 2601, Australia.

---

*To whom correspondence should be addressed. Present address: Department of Ecology and Evolution, University of Chicago, Chicago, IL 60637.